Electric Power Systems Research 214 (2023) 108792

Contents lists available at ScienceDirect

Electric Power Systems Research

journal homepage: www.elsevier.com/locate/epsr

Energy management and operational planning of renewable energy resources-based microgrid with energy saving

Tao Hai [a,b,c], Jincheng Zhou [a,b,*], Kengo Muranaka [d]

[a] School of Computer and Information, Qiannan Normal University for Nationalities, Duyun, Guizhou 558000, China
[b] Key Laboratory of Complex Systems and Intelligent Optimization of Guizhou, Duyun, Guizhou 558000, China
[c] Institute for Big Data Analytics and Artificial Intelligence (IBDAAI), Universiti Teknologi MARA, Shah Alam, Selangor 40450, Malaysia
[d] Solar Energy and Power Electronic Co., Ltd, Tokyo, Japan

ARTICLE INFO

Keywords:
Resource scheduling
Hybrid HWOA-PS algorithm
Stochastic programming
Energy storage systems
Photovoltaic

ABSTRACT

Energy resource scheduling is one of the major problems in power systems. This issue has become even more significant as renewable sources with intermittent power output are becoming more and more prevalent. Due to their low environmental impact and low operating costs, renewable energy sources (RESs) have attracted interest. The excess power generated by such generation methods may be a negative that affects power systems, hence issues relating to such systems should be properly handled. The optimal operation of a microgrid (MG) with several distributed generation (DG) units and uncertain behavior of RESs is suggested in this research using a stochastic optimization approach. So, for an MG fitted with a solar photovoltaic (PV) unit, this research proposes a day-ahead scheduling paradigm. In this regard, the effects of various climatic circumstances on the power production of the PV unit and the optimal scheduling of the MG have been examined in this research. In order to achieve this, statistics on solar irradiance were extracted from four distinct days from each of the four seasons. The single-objective optimization framework used to design the scheduling problem states that the objective function should be to minimize the total operating cost across the scheduling period. The aforementioned day-ahead scheduling problem can be solved by the "hybrid whale optimization algorithm and pattern search (HWOA-PS)" optimization algorithm, while both renewable and nonrenewable generating units, as well as an energy storage system are present. In order to confirm the higher performance of the recommended approach, a thorough comparison between the Hybrid WOA-PS algorithm and a few well-known optimization algorithms has also been conducted.

1. Introduction

Renewable energy sources (RESs) have the capability to offer energy systems with net-zero carbon energy addressing the worldwide concerns surrounding climate change [1,2]. RESs mainly comprise wind energy, solar energy, hydro, geothermal, and hydrogen energy, among others. In this regard, PV systems, WTs, and FCs are utilized as efficient energy harvesting and delivery technologies. Microgrids (MGs) have already been implemented and operated in the power system's low-voltage (LV) sector [3,4], addressing the question of how to integrate these technologies into the power system. An MG largely consists of renewable energies, electric vehicles as mobile storage systems, and active loads, besides stationary storage devices [5]. It can provide the required services while tied/untied to/from the utility grid [6]. This issue has become a critical issue in power systems [7] because the quality of service provided by the MG mainly depends upon the properly scheduling of resources. In general, the mentioned problem is constrained by the operational limitations of the generating units and input uncertainties needing efficient characterization tools.The volatile WT and PV generation, dynamic load demand, and the ambient temperature would be accounted for as the important uncertain parameters impacting the optimal operation of MGs. Accordingly, an efficacious tool would be needed for coping with such severe uncertainties. Intermittency of renewable power generation would entail an extra operating cost. The energy, harvested by PV panels can be utilized for various purposes, such as district heating and feeding load demands [8].

* Corresponding author at: School of Computer and Information, Qiannan Normal University for Nationalities, Duyun, Guizhou 558000, China.
E-mail address: guideaaa@126.com (J. Zhou).

https://doi.org/10.1016/j.epsr.2022.108792
Received 22 April 2022; Received in revised form 28 July 2022; Accepted 4 September 2022
Available online 27 September 2022
0378-7796/

Nomenclature

RES	renewable energy sources
MGs	microgrids
PV	photovoltaic
HWO	hybrid whale optimization
PS	pattern search
WTs	wind turbines
FCs	fuel cells
LV	low-voltage
MTs	microturbines
EES	electrical energy storage
DERs	fistributed energy resources
PSO	particle swarm optimization
DNI	direct normal irradiance
DR	demand response
SOC	state of charge
PCC	point of common connection
PDF	probability distribution function
GA	genetic algorithm
ICA	differential evolution
SFLA	shuffled frog-leaping algorithm
V_{pv}	output voltage
I_{pv}	output current
NREL	National Renewable Energy Laboratory
I_{ph}	photocurrent
R_{sh}	shunt resistance
n	ideality factor
R_s	series resistance
I_{PVO}	saturation current
B_{Gi}	bid of DG
B_{sj}	bid of BESS
S_{sj}	start-up cost
S_{Gi}	shutdown cost

1.1. Literature review

In Ref. [9], a model for the bidding strategy of large customers equipped with RESs, microturbines (MTs), and storage devices is presented. Uncertainties in RES generation, load demand, and market price are all acknowledged as having significant implications for operational planning. In Ref. [10], a for-profit business plan for PV and electrical energy storage (EES) systems in the private residential sector was developed to compete in the Italian energy market. In Ref. [11], a trustworthy energy management system for concurrent PV, FC, and WT operation is proposed. Using a diesel generator, a WT, and solar panels together is one solution to the integration challenge of DGs discussed in Ref. [12], with the goal of keeping costs down.

Many research works have thus far been devoted to developing energy management tools for MGs using metaheuristics algorithms and multiobjective optimization frameworks. Such techniques have well been established in solving complex optimization problems such as the day-ahead MG's operation due to their local and global search capabilities. In this regard, Refs. [13,14] have used a technical and economic analysis of how distributed energy resources (DERs) impact the MG's operation and system losses, intended to minimize the system cost and environmental emissions. An approach using the fuzzy self-adaptive PSO has been deployed in [15] to tackle the economic-environmental scheduling of DERs within an MG. The adaptive enhanced PSO has been employed in [16] for the resource scheduling of an MG with high renewable power generation and battery energy storage system, besides a fuel cell (FC) unit and a microturbine. The combined heat and power scheduling problem has been addressed in [17] within a two-objective optimization model aimed at concurrently optimizing the system's operating cost and emissions where there are thermal units and storage systems besides demand response programs (DRPs). An artificial intelligence-based energy management system has been introduced in [18] for concurrently minimizing the total operating cost and emissions of an MG. Ref. [19] employed the genetic algorithm (GA) to tackle an islanded MG sizing problem through a multiobjective optimization model seeking to minimize emissions and lifecycle cost while maximizing renewable power integration. A short-term scheduling model has been developed in [20] to optimally address the day-ahead operation problem of an MG in the presence of high renewable power generation, a battery, and also DRPs and it has been concluded that the emissions can be significantly mitigated using the presented model.

A stochastic mixed-integer linear programming (MILP) framework is suggested in [21] to optimally design and plan an MG including combined heat and power (CHP) units using the Monte-Carlo simulation technique. A model on the basis of a hetero-functional graph theory rooted in the axiomatic design is used in [22] for presenting an effective MG operation that is dynamic. A MILP-based model has been proposed in [23] for the optimal operation of an MG to minimize the operating cost. The MG comprises different generation technologies from microturbines (MTs) and fuel cells (FCs) to wind turbines (WTs) and solar PV panels. In this respect, the studied MG is separated into multiple areas and the MG can inject power into the upstream network. An MG intended to serve residential loads is presented in [24], where an optimal energy management system has been proposed to schedule the generating units, including combined cooling, heat and power (CCHP), PEVs, PV panels, and storage systems of battery type. The proposed problem is based on the stochastic scenario-based approach and the uncertain parameters have been characterized using the probability distribution functions (PDFs). The normal PDF has been used for the load demand, while for the electrical and heat load demand the Weibull PDF has been utilized. Solar irradiance has also been modeled using the Beta PDF. As the number of generated scenarios is too high, a scenario reduction technique is used. A multi-layer method is proposed in [25] for scheduling a smart distribution network (SDN), while it is comprised of multiple MGs (MMGs).

Power losses must be reduced, and efficient placement of EES systems in distribution networks has been discussed previously [26]. In Ref. [27], a comprehensive energy management framework for an isolated MG was designed. This framework takes into account the many different types of distributed energy resources (DERs) that might be present. Ref. [27] provides more information about how MGs might be used effectively when on the island mode. In Ref. [28], an optimization model was developed with the goal of minimizing the total cost while to manage the optimal operation of MGs equipped with DERs, a linear programming (LP) model is used in Ref. [29]. The planning problem of MGs with DERs is addressed with an MILP approach in Ref. [30]. For the coordinated day-ahead operation of interconnected MGs, Ref. [31] outlined a hierarchical control technique. It is important to note, however, that the PSO method is capable of being used to predict the parameters of the solar PV generation system, as one of the uncertainty sources in the day-ahead operating problem [32]. In order to specify the operating points of a CHP system and other generation assets in an MG, a bi-objective optimization model has been proposed in [33] aimed at simultaneously reducing operating costs and environmental emissions. With similar objectives, Ref. [34] presents an intelligent energy management paradigm for an MG outfitted with RESs with parameter uncertainty. In Ref. [35], an LP technique is used to examine how DR programs could be used in the day-ahead management of an MG. The self-scheduling mechanism depicted in Ref. [36] was implemented by an MG in Taiwan to maximize profits while mitigating emissions. In

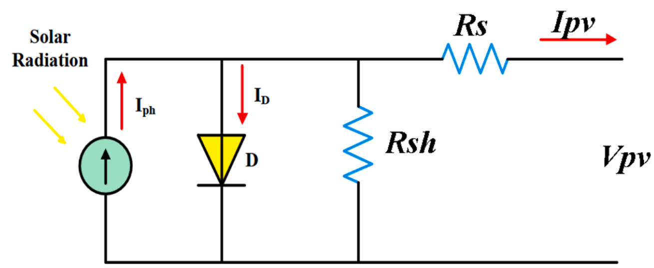

Fig. 1. The circuit representation of the proposed photocell model.

Ref. [37], a chaotic quantum genetic algorithm (CQGA) was used to solve the MGs-DGs resourced economic-environmental power dispatch problem. The Whale optimization algorithm is another optimization algorithm, inspired by nature, i.e. humpback whales' hunting technique, the so-called bubble-net feeding approach. In this respect, the whales produce bubbles and surround the prey by these bubbles through a spiral movement and move toward the surface [35]. A combinatorial optimization algorithm based on the squirrel search algorithm and WOA, known as "SSAWO" has been utilized in Ref. [36] to tackle the power flow management of a grid-connected hybrid generation system. The WOA ensures locating the online control signals by employing the parallel execution for the variations of the active and reactive power. An optimal battery EES (BEES) system allocation technique has been developed in Ref. [37] based on the single-objective optimization model, aimed at optimizing power losses. A multi-objective WOA has been used for the allocation of charging stations for plug-in electric vehicles together with PV and BEES systems in distribution networks [38].

As was indicated before, the optimal operation of MGs is complicated by a number of sources of uncertainty, including load demand and variable power supply from RESs. Stochastic programming is an effective method for this purpose. In particular, household installations of solar photovoltaic panels (PVs) have an impact on the efficiency of distribution networks and, in particular, on the performance of MGs. Consequently, applying various PV power generation realizations and evaluating their effects on the ultimate operating strategy can be accomplished with scenario-based optimization. For this reason, this work models various levels of solar irradiation while accounting for seasonal changes in weather patterns. The investigated MG consists of a WT, solar panels, an FC, a battery energy storage system, and an MT.

The current paper delves into the question of how best to plan for the next day's use of MG, involving a solar PV panel and other DERs. The suggested framework accounts for seasonal variations in weather by simulating conditions on a single day in each season. The best possible resource schedule and, by extension, the lowest possible operating cost, could then be calculated. Stochastic programming is used here with the BEES system's state-of-charge set to zero while assets can be turned on and off at will. It is also worth noting that the RESs would be used at their full potential and that the issue of load demand uncertainty is taken into consideration. The "HWOA-PS" (hybrid WOA and PS) is then used to tackle the resulting optimization problem. Note that the WOA and PS would conduct the global search and the local search, respectively. The main contributions of the papers are as below:

- Modeling and using the effects of seasonal weather conditions.
- Proposing an effective day-ahead resource scheduling framework for a grid-connected MG.
- Using real data to assess the developed model for the PV system.

It is also worth mentioning that the remainder of the paper is categorized as follows, where the next section includes the model, presented for the PV system. The third section proposes the energy scheduling model, while the descriptions of the stochastic programming and the applied HWOA-PS would be available in Sections 4 and 5, respectively. The results, derived by simulating the day-ahead operation problem are

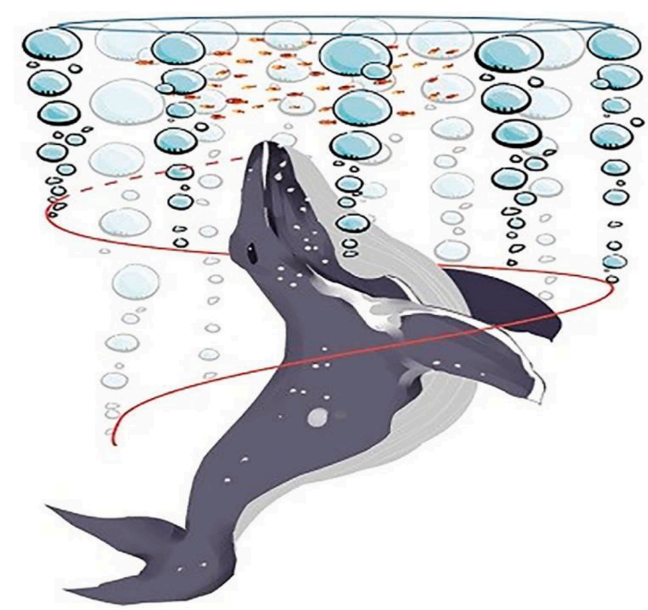

Fig. 3. Humpback whale and its bubble-net hunting technique.

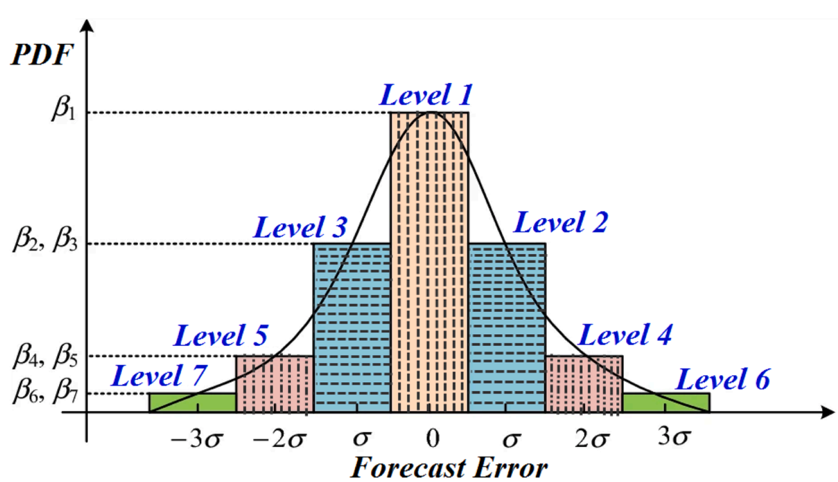

Fig. 2. A typical discretized PDF.

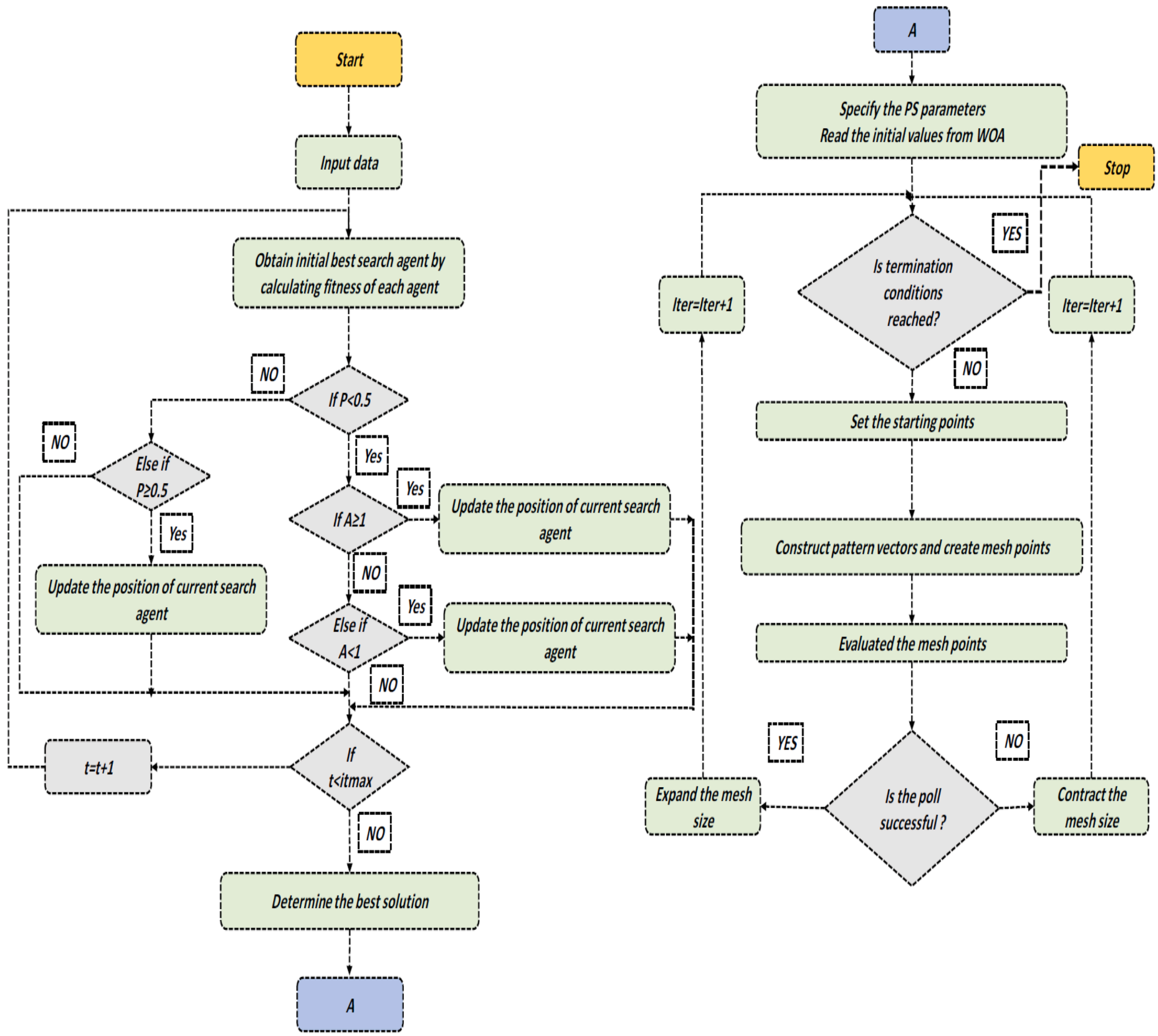

Fig. 4. Flowchart of the HWOA-PS.

given in Section 6 and conclusion remarks have been represented in Section 7.

2. PV model

PV panel is formed by several cells that are connected to each other. The interconnection would be in parallel and series to achieve the desired values of current and voltage. Although there are different structures for the PV panel, a single-diode model which is of high accuracy is employed in this paper to prevent any more complexities [39]. As may be seen in Fig. 1, this setup is depicted schematically for a single photocell. The PV system's I-V equation can be written as (1). Adding series and parallel connections, respectively, can produce the necessary output voltage and current. Many PV modules are wired together to form the whole panel [40].

$$V_{PV} = \frac{nKT}{q} \ln\left(\frac{I_{ph}}{I_{PV}} + 1\right) \tag{1}$$

$$I_{PV} = I_{ph} - I_{PV0}\left[\exp\left(\frac{q(V_{PV} + I_{PV}R_s)}{nKT} - 1\right)\right] - \frac{V_{PV} + R_s I_{PV}}{R_{sh}} \tag{2}$$

Where R_s and R_{sh} are the series and shunt resistances used in the model, respectively. Moreover, the ideality factor of the p-n junction diode is represented by the symbol n, and its photocurrent, I_{ph}, is measured in Ampere. In addition, I_{PVO}, or reserve saturation current, is calculated in Amperes and K, or the Boltzmann constant is displayed as 1.38×1023 J/K. In addition, q, the electronic charge, is set to be 1.602×1019 C. The model is next subjected to the photocell's temperature, denoted as T, in Kelvin. If the fill factor, current, and voltage were all increased to their maximum values, the system's nominal capacity would be available at the output. Maximizing the fill factor requires setting the series resistance to zero and the shunt resistance to infinity, respectively.

3. Objective functions

As previously mentioned, an MG is equipped with DERs. The operation of MGs is exposed to several uncertainties, mainly due to volatile renewable power generation, load demand, as well as market price. These uncertainties impose additional costs on the system and in some cases, cause power shortage when supplying the local load demand. One possible and economical solution is to connect the MG to the upstream

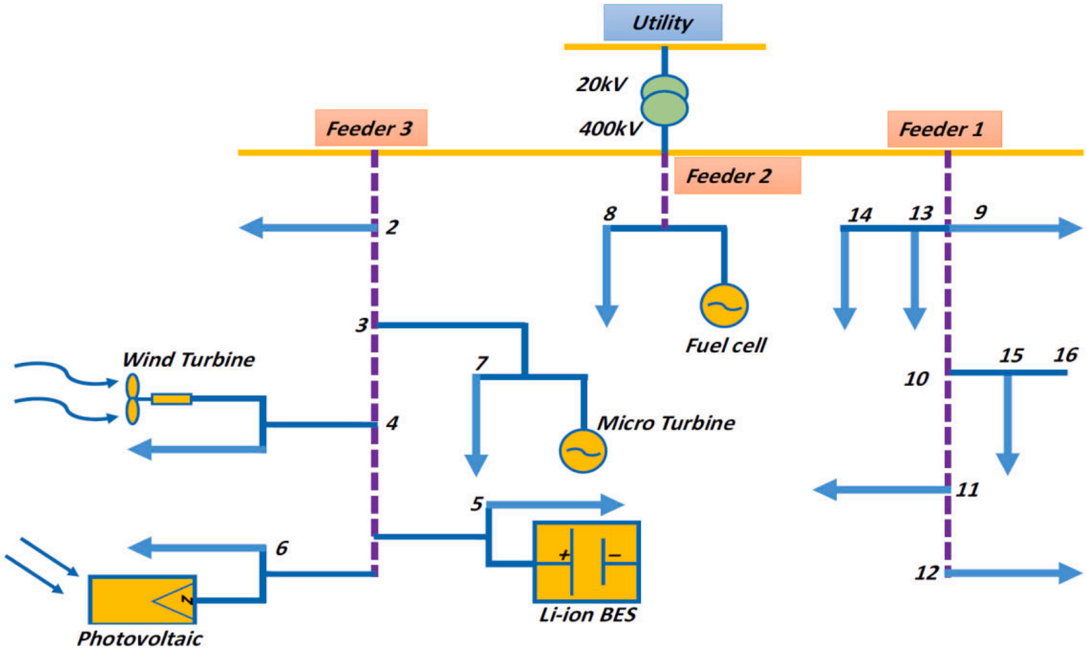

Fig. 5. The microgrid test system.

Table 1
Characteristics of the studied PV panel (MF165EB3 by Mitsubishi Electric).

I_{sc}	V_{oc}	V_{mpp}	I_{mmp}	n_s
7.36A	30.4 V	24.2 V	6.83 A	50

Table 2
Price of DGs [7, 8].

	Bat	PV	WT	Bat	FC	MT
P_{Min} kw	-30	0	0	-30	3	6
Bid €ct/kwh	0.38	2.584	1.073	0.38	0.294	0.457
P_{Max} kW	30	25	15	30	30	30
SUD/SDC €ct	–	–	–	–	1.65	0.96

system to transact power when necessary. By formulation, the total cost can be written as below [32,17]:

$$Min\, f(X) = \sum_{t=1}^{T} \mathrm{Cost}^t = \sum_{t=1}^{T}\left\{\sum_{i=1}^{N_g}[u_i(t)p_{Gi}(t)B_{Gi}(t) + S_{Gi}|u_i(t) - u_i(t-1)|]\right\} + \sum_{j=1}^{N_s}\left[u_j(t)p_{sj}(t)B_{sj}(t) + S_{sj}\left|u_j(t) - u_j(t-1)\right|\right] + p_{Grid}(t)B_{Grid}(t)u_j(t) \tag{3}$$

where P_{Grid} (t) is the active power that is purchased from or sold to the utility at time t and B_{Gi} (t) is the utility's bid at *t*. S_{Gi} and S_{sj} are the start-up and shut-down costs, respectively. Active powers of units and their associated states are included in the vector of state variables known as X, which is defined as follows [14]:

$$X = [P_g, U_g]_{1\times 2nT}; P_g = [P_G, P_s]; \quad n = N_g + N_s + 1 \tag{4}$$

where P_g and N_g are the active power and total number of all DG units, respectively. N_s is the total number of storage units, *T* is the total number of hours in the time period under consideration, *n* is the number of state variables. Additionally, $P_{Gi}(t)$ and $P_{sj}(t)$, respectively, demonstrate the active power of DG units and energy storage systems. These variables fit the following descriptions:

$$\begin{aligned} &P_G = [P_{G,1}, P_{G,2}, ..., P_{G,N_g}]; \quad P_s = [P_{s,1}, P_{s,2}, ..., P_{s,N_s}] \\ &P_{G,i} = [P_{G,1}(1), P_{G,2}(2), ..., P_{G,i}(T)]; \quad i = 1,2,...,N_{g+1} \\ &P_{s,j} = [P_{s,j}(1), P_{s,j}(2), ..., P_{s,j}(T)]; \quad i = 1,2,...,N_s \end{aligned} \tag{5}$$

3.1. Power balance

The fundamental requirement for managing a power system's operation is to meet the load with the available generations. where N_L is the total number of load levels and $P_{L,l}$ is the magnitude of the *k*th load.

$$\sum_{i=1}^{N_g} P_{G,i}(t) + \sum_{i=1}^{N_s} P_{s,j}(t) + P_{Grid}(t) = \sum_{l=1}^{N_L} P_{L,l}(t) \tag{6}$$

3.2. Generation limitations

The permissible operating range must be met by the power produced by the generation units, the power exchanged with the upstream grid, and the power of the BEES system.

$$\begin{aligned} &P_{Gi,\min}(t) \le P_{Gi}(t) \le P_{Gi,\max}(t) \\ &P_{grid,\min}(t) \le P_{Grid}(t) \le P_{grid,\max}(t) \\ &P_{sj,\min}(t) \le P_{sj}(t) \le P_{sj,\max}(t) \end{aligned} \tag{7}$$

Table 3
The forecasted WT.

Hour	WT (kW)
1	1.785
2	1.785
3	1.785
4	1.785
5	1.785
6	0.9140
7	1.785
8	1.308
9	1.785
10	3.085
11	8.772
12	10.413
13	3.923
14	2.377
15	1.785
16	1.302
17	1.785
18	1.785
19	1.302
20	1.785
21	1.302
22	1.302
23	0.9140
24	0.6120

Table 4
Solar irradiance profile.

Hour	GHI(W/m2)				DNI(W/m2)			
	HS	CS	HC	CC	HC	CS	HC	CC
1	0	0	0	0	0	0	0	0
2	0	0	0	0	0	0	0	0
3	0	0	0	0	0	0	0	0
4	0	0	0	0	0	0	0	0
5	0	0	0	0	0	0	0	0
6	32	0	5	0	166	0	2	0
7	172	0	71	0	624	0	16	0
8	388	67	172	12	802	548	27	0
9	608	251	340	73	893	882	81	1
10	805	434	381	134	949	979	51	0
11	959	566	480	187	982	1008	69	2
12	1049	650	405	221	992	1032	12	2
13	1080	671	367	237	995	1027	9	0
14	1061	624	426	196	1003	1027	15	1
15	960	523	329	146	982	1012	5	1
16	807	357	225	91	950	925	2	1
17	617	165	152	22	906	774	1	0
18	397	34	88	0	821	226	1	0
19	175	0	24	0	636	0	1	0
20	34	0	1	0	175	0	1	0
21	0	0	0	0	0	0	0	0
22	0	0	0	0	0	0	0	0
23	0	0	0	0	0	0	0	0
24	0	0	0	0	0	0	0	0

where the minimum active powers of the *i*th DG, the *j*th storage, and the utility at time t are $P_{G,\min}(t)$, $Ps,\min(t)$, and $P_{grid,\min}(t)$, respectively. $P_{G,\max}(t)$, $P_{s,\max}(t)$, and $P_{grid,\max}(t)$ are the maximum power outputs of the associated units at hour *t*, respectively.

The above constraints are checked at every iteration of the solution procedure and if any violation occurs for the value of the variable, in case it is more than the maximum value, its value is assigned to the problem as its maximum amount. On the contrary, if the value of the variable is lower than the minimum permitted limit, its value is assigned to the problem as its minimum limit.

3.3. Energy storage limit

The following equation and restriction can be written as a result of the limitation on the charge and discharge rate of storage devices during each time interval:

$$W_{ess}(t) = W_{ess}(t-1) + \eta_{charge}\Delta t - \frac{1}{\eta discharge}P_{discharge}\Delta t \tag{8}$$

$$\begin{cases} W_{ess,\min} \leq W_{ess}(t) \leq W_{ess,\max} \\ P_{charge}(t) \leq P_{charge,\max} \\ P_{discharge}(t) \leq P_{discharge,\max} \end{cases} \tag{9}$$

Where P_{charge} and $P_{discharge}$ are the allowed rates of charge and discharge over a specific time Δt, $W_{ess,t}$ and $W_{ess,t-1}$ are the amounts of energy storage of the battery at time slot *t* and time slot $t-1$, respectively. Moreover, the efficiencies in the charging and discharging modes are denoted by η_{charge} and $\eta_{discharge}$, respectively. The battery energy storage limits are $W_{ess,\min}$ and $W_{ess,\max}$ while the maximum rates of charge or discharge are $P_{charge,\max}$ and $P_{discharge,\max}$ for each interval of time Δt.

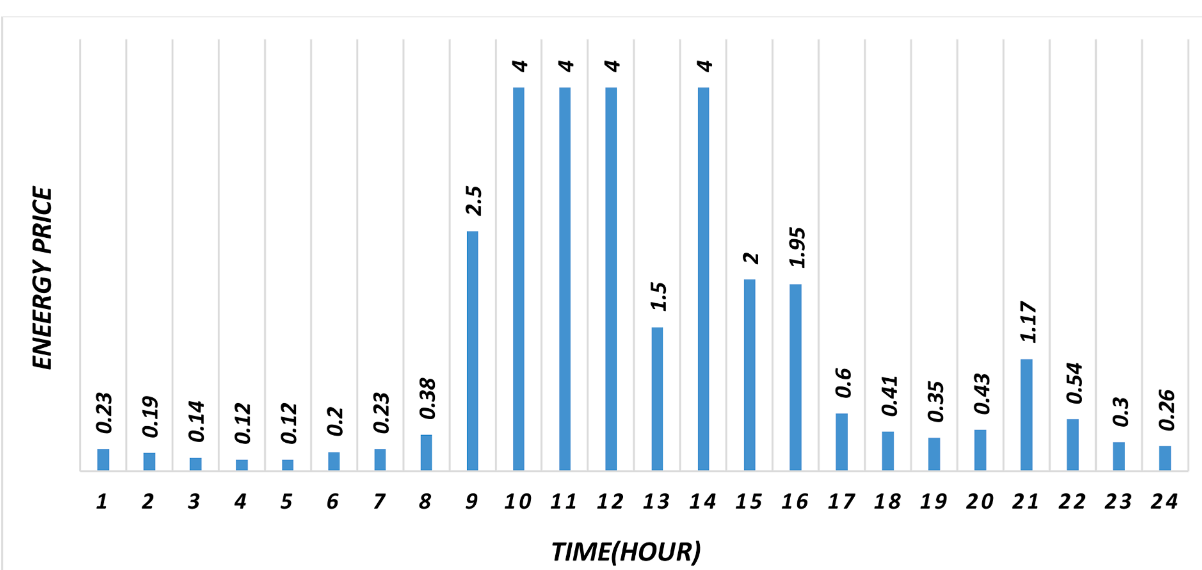

Fig. 6. Market price.

Table 5
Solar irradiance profile.

Hour	Diff (W/m2)				T (°C)			
	HS	CS	HC	CC	HC	CS	HC	CC
1	0	0	0	0	–	–	–	–
2	0	0	0	0	–	–	–	–
3	0	0	0	0	–	–	–	–
4	0	0	0	0	–	–	–	–
5	0	0	0	0	–	–	–	–
6	15	0	5	0	24.4	–	27.8	–
7	35	0	68	0	25.6	–	28.9	–
8	53	12	162	12	27.8	-18	30	0
9	70	22	294	73	31.7	-10	31.7	0
10	84	31	343	134	33.9	-1.7	31.7	0
11	93	38	419	187	35	-0.6	33.3	0
12	98	42	393	220	36	1.7	32.8	0
13	101	49	358	237	37.2	2.2	32.2	0
14	99	41	411	196	38.3	3.3	32.2	0
15	93	35	325	145	38.9	1.7	32.8	0
16	84	31	223	91	39.4	1.1	32.2	−6
17	71	20	151	22	39.4	−3.9	32.2	−6
18	53	9	88	0	38.9	–	31.1	–
19	35	0	24	0	38.3	–	30.6	–
20	15	0	1	0	36.1	–	29.4	–
21	0	0	0	0	–	–	28.9	–
22	0	0	0	0	–	–	–	–
23	0	0	0	0	–	–	–	–
24	0	0	0	0	–	–	–	–

4. Uncertainties based on scenario generation

A number of variables, including load demand, renewable power output, and market price, are known to cause fluctuations in the solution to the problem. For this reason, this article uses a scenario-based stochastic optimization method [41] to effectively define the unknown parameters in the context of a day-ahead operating problem. Here, the roulette wheel is used to generate the necessary number of scenarios for each parameter's uncertainty level in the range [0, 1]. Similarly, the PDF of the unknown parameter is discretized, and the probability of each possible value is calculated. The PDF has been discretized across seven intervals. Fig. 2 is a commonly encountered discretized PDF.

5. Hybrid WOA-PS algorithm

The pattern search (PS) method has already been introduced as a derivative-free technique with straightforward implementation and high efficiency. This algorithm utilizes a well-designed operator to improve the global and local search capabilities. The points, used by this method can either approach the best point or not. The PS algorithm starts with using a set of points, named "mesh", around the initial points, generated by the WOA. The mesh is generated by adding the current points to a scalar multiple of a set of vectors, named "pattern". An initial point with a more desired value of objective would turn into the initial point in the subsequent iteration. After that, the PS algorithm is utilized for fine-tuning the most desired solution, obtained from the WOA. The values, initially derived from the WOA would be utilized for the initialization of the PS.

Table 6
Comparative results (Hot sunny day).

Algorithm	Best	Worst	Average	Std
GA	359.6832	394.7913	386.3245	18.4458
PSO	358.0602	391.4875	382.1487	17.0214
DE	357.0241	390.1784	380.2478	16.0214
ICA	355.3221	388.9643	378.1178	14.9514
SFLA	353.1282	387.3317	.376.9514	14.0741
Hybrid WOA-PS algorithm	351.1964	385.1351	375.7415	12.2241

5.1. The whale algorithm

The WOA was first developed by Mirjalili and Andrew Lewis in the year 2016, inspired by the hunting technique, used by the humpback whales [35,36,42]. This type of whale goes in-depth of around 12 m and through a spiral movement toward the surface, producing bubbles of different sizes. These bubbles encompass the prey, close to the surface and form a concentration of prey. After that, by opening up the mouth, the humpback whale eats the food. In this regard, the WOA is based on three principles by mimicking the spiral bubble net mechanism, used by the whale. The first one is the spiral movement technique, the second one is random hunting, and the third one is the encompassment. The net of bubbles, produced by the whale to encompass the prey is illustrated in Fig. 3. This method is mathematically modeled in the subsequent sub-sections.

5.1.1. Encircling prey

The humpback whales are capable of remotely locating the prey and

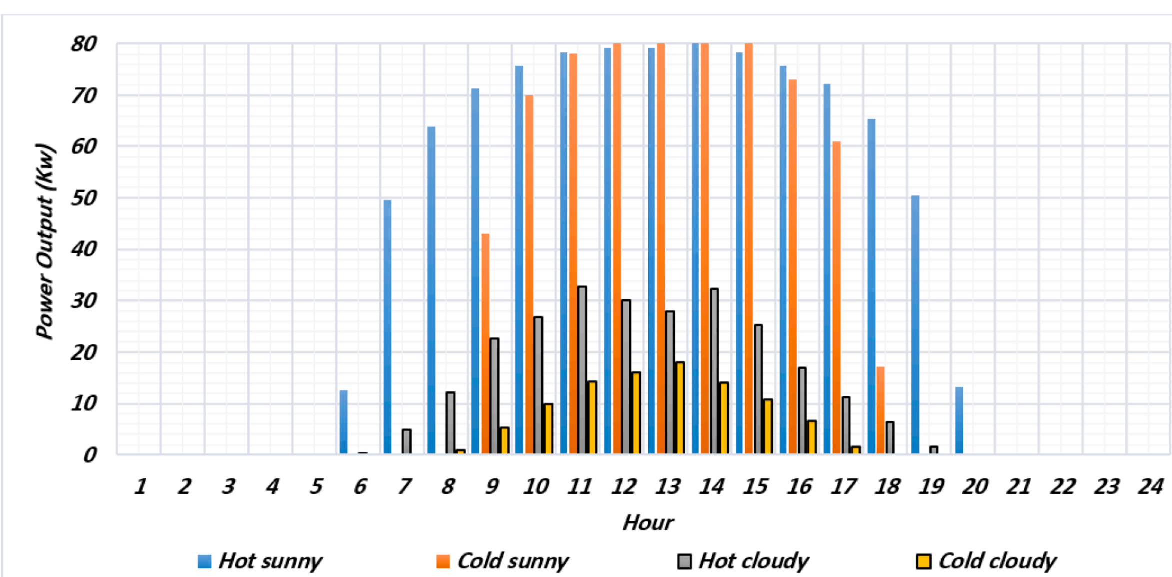

Fig. 7. Power output for different seasons.

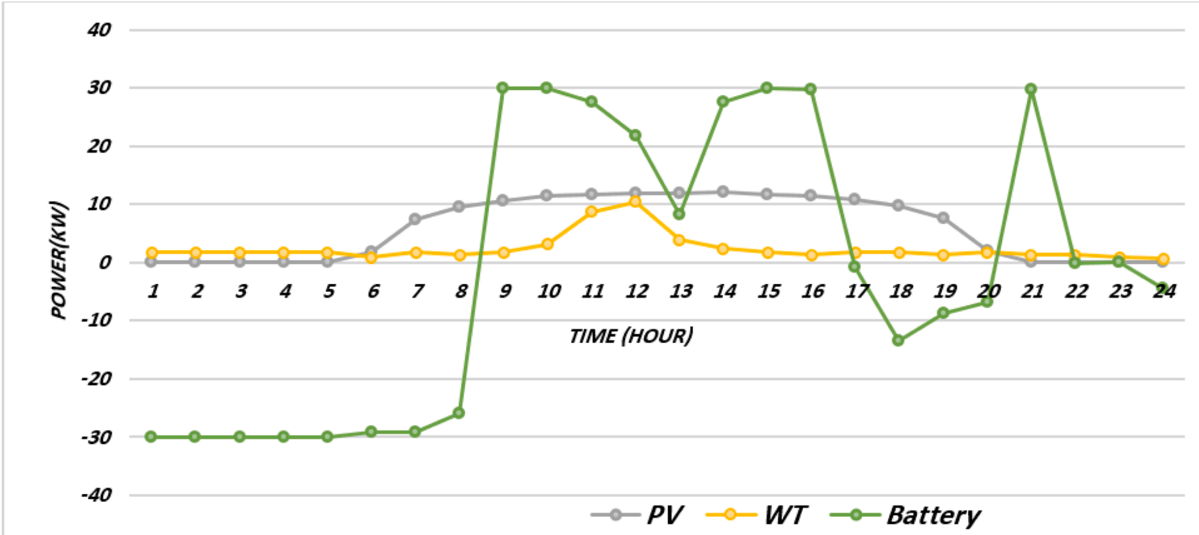

8(a)

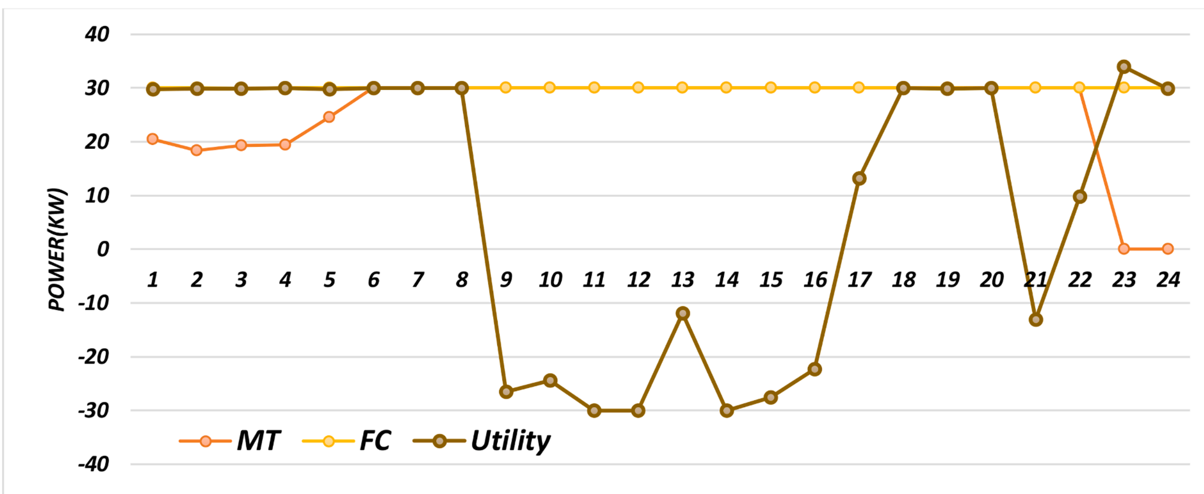

8(b)

Fig. 8. (a) and (b). Hourly dispatch results, reported by the HWOA-PS algorithm (Hot sunny day); (c) Battery's charging/discharging; (d) Mean simulation time.

encompassing them to hunt. The WOA supposes that the optimal location in the present population is the prey. Then all whales encompass the prey and the location is modified by utilizing relationships (10) and (11), in which the iteration is shown by t, and the vectors of coefficients are shown by A and C and stated as (12) and (13), respectively. It should be noticed that the most desired position within the present population is denoted by $X^*(t)$.

$$D = |CX^*(t) - X(t)| \tag{10}$$

$$X(t+1) = X_{rand} - A \times D \tag{11}$$

$$A = 2ar_1 - a \tag{12}$$

$$C = 2r_2 \tag{13}$$

Where, the random values r_1 and r_2 should be within the interval [0 1]. Besides, α reduces from 2 to zero, while the number of iterations is shown by T_{max}.

5.1.2. Spiral bubble-net feeding maneuver

By using Eq. (14), the spiral movement of the whale toward the optimal member is modeled.

$$X(t+1) = X*(t) + D_p e^{bl}\cos(2\pi l) \tag{14}$$

It is noted that the distance between the optimal member, shown by X, prior to the update and the optimal location, X_{best}, is determined by $D_p = |X^*(t) - X(t)|$. Furthermore, b shows a constant, modeling the spiral movement and l indicates a random value that falls within the interval [−1 1]. The position of every individual whale is specified by relationship (14).

5.1.3. Searching for prey

The hunting and searching process is carried out in a random way based on the location of the whale. The location of each whale is updated by using the following equations in the WOA, where the randomly chosen vector of whale positions is denoted by X_{rand}.

$$D = CX_{rand} - X(t) \tag{15}$$

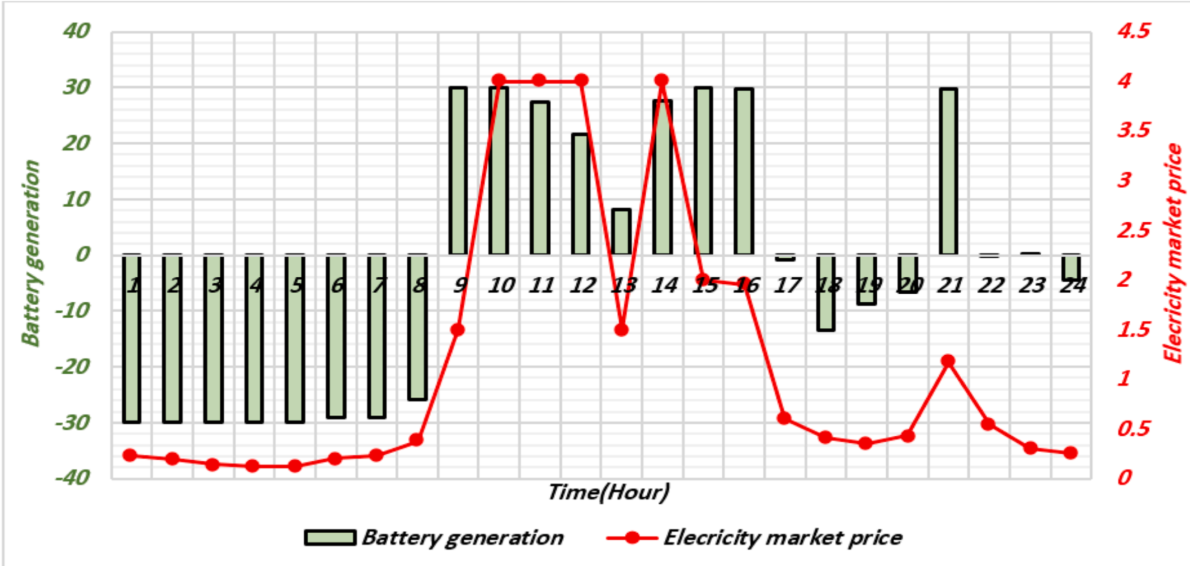

8(c)

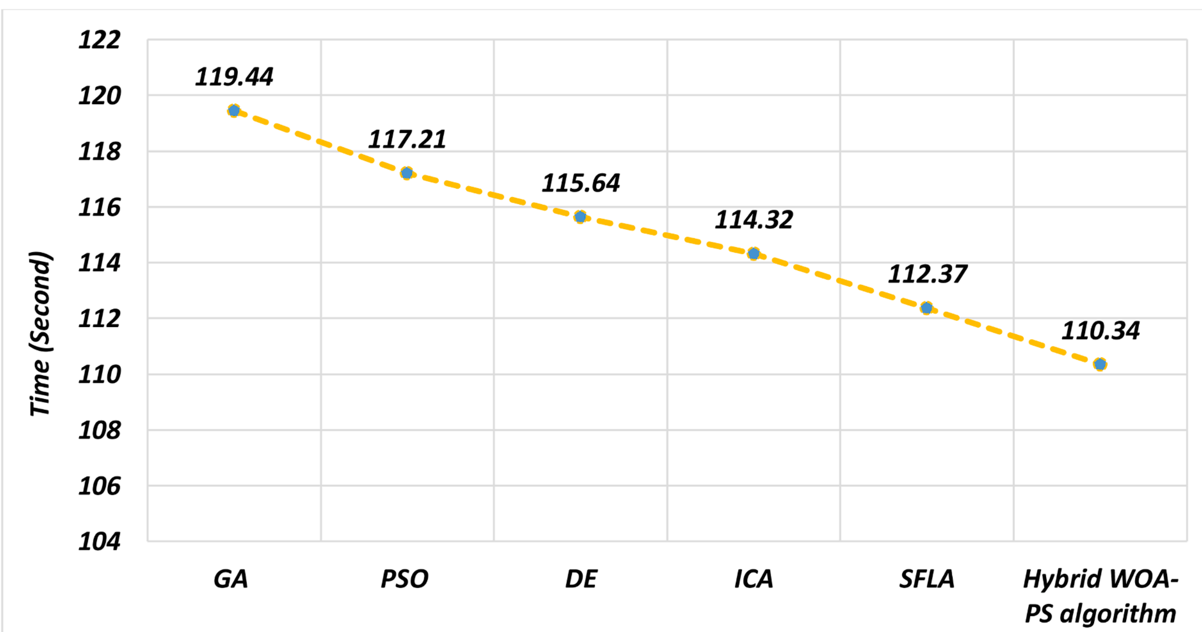

8(d)

Fig. 8. (*continued*).

Table 7
Comparative results (Cold sunny day).

Algorithm	Best	Worst	Average	Std
GA	294.6581	371.3715	338.212	40.1542
PSO	291.7038	366.7519	334.215	32.1232
DE	290.0982	364.1754	334.0136	30.6548
ICA	288.0325	363.0451	330.9784	29.8541
SFLA	287.1478	362.9473	328.7496	28.3349
Hybrid WOA-PS algorithm	284.2851	360.1147	325.334	27.5147

$$X(t+1) = X_{rand} - A \times D \tag{16}$$

5.2. *Pattern search algorithm (PS)*

5.2.1. *Overview*

The PS algorithm is classified into evolutionary ones and it has thus far been applied to solve a wide range of optimization problems [43,44], with proven efficiency and effectiveness, once combined with other algorithms. The present paper employs this algorithm for the local search process, and jointly with the WOA.

5.2.2. *Search mechanism*

The procedure, described below shows the structure of the search technique [43].

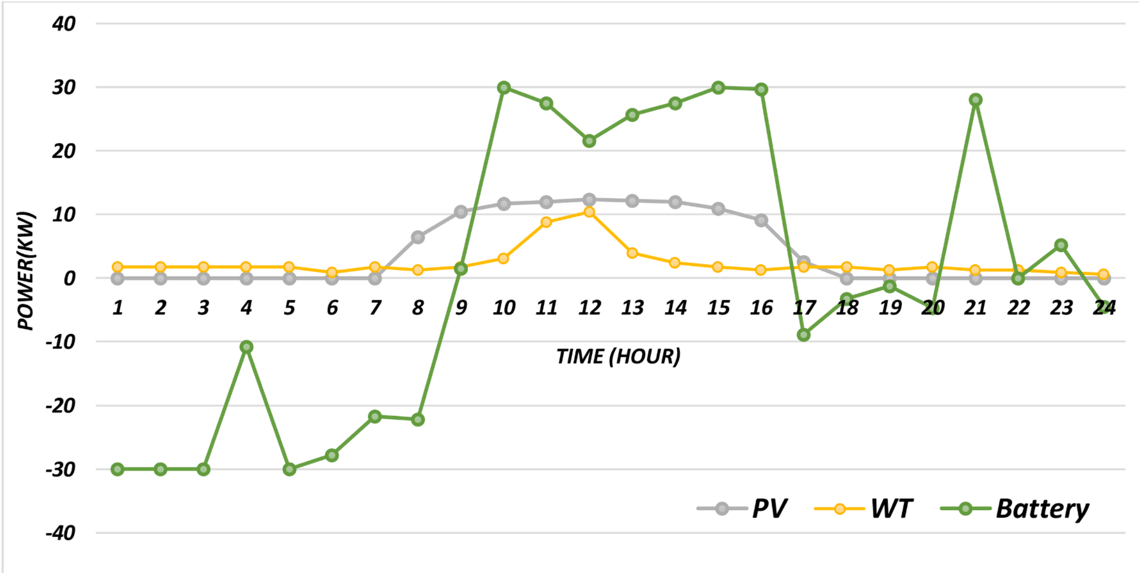

9 (a)

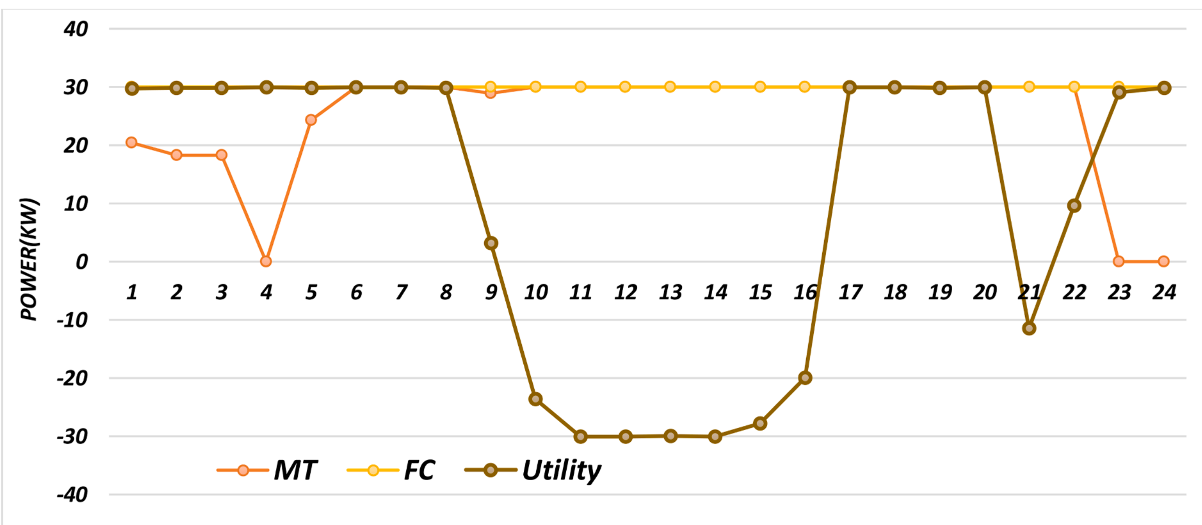

9(b)

Fig. 9. (a) and (b). Hourly dispatch results, reported by the HWOA-PS algorithm (Cold sunny day); (c) Battery's charging/discharging; (d) Mean simulation time.

1 Firstly, a set of points, named mesh is generated around the initial point, indicated by X_0. The vectors of direction are also [1 0], [0 1], [−1 0], [0 − 1].
2 The mesh is constructed when the current point is added to a scalar multiple of a set of vectors, named "pattern". By using the PS algorithm, the vectors of direction are added to the initial point X_0 and these mesh. By assessing every point in the mesh with respect to the value of the objective function, the current point is used as the new point for the subsequent generation, provided that the value of the objective function is enhanced.
3 The termination conditions for this approach are as below:

3.1. The size of mesh becomes smaller than the direction accuracy.
3.2. Achieving the maximum number of iterations.

The proposed method is demonstrated in Fig. 4.

6. Results

The MG, studied in this paper is equipped with MT, a BEES system, a PV, and a WT, besides an FC. Furthermore, as Fig. 5 depicts, the load demand comprises three sectors, commercial, industrial, and residential loads [28,14]. The period of scheduling is 24 h on an hourly basis and the assumptions of the problem are as follows: firstly, only the real power generation of assets is considered; secondly, power transaction is allowed between the MG and the upstream network. Moreover, the unknown parameters, represented in Table 1 have been estimated using the Gauss-Seidel approach. The total load demand is 80 kW.

The techno-economic data of DGs and upstream grid are represented in Table 2. The cost of using WT and PV panels is significantly lower than other units, which turns them into appropriate options to supply the load demand. Also, the hourly forecasts of power outputs of WT and market price are indicated in Table 3 and Fig 6 respectively.

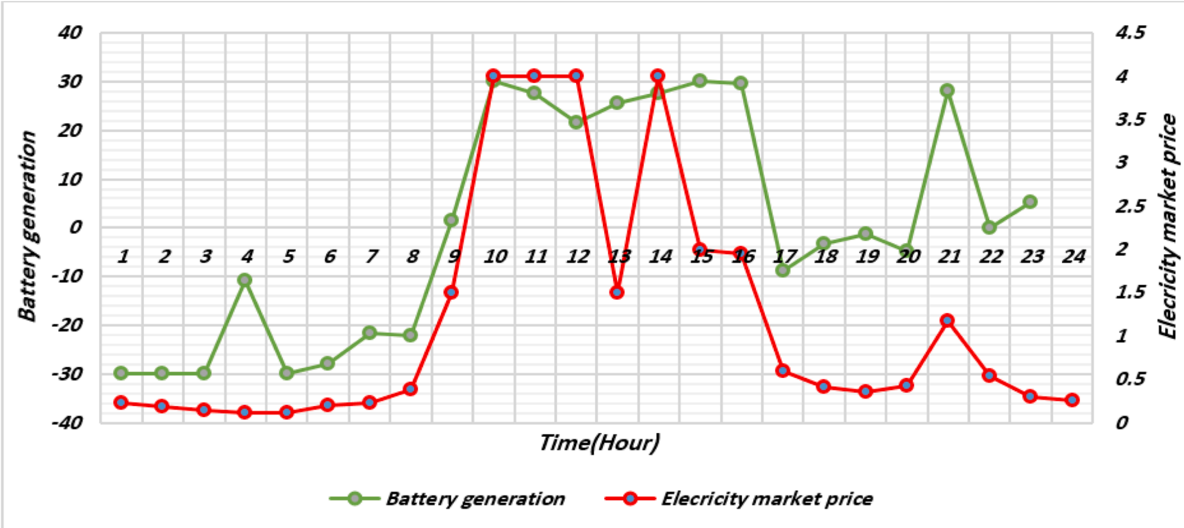

9(c)

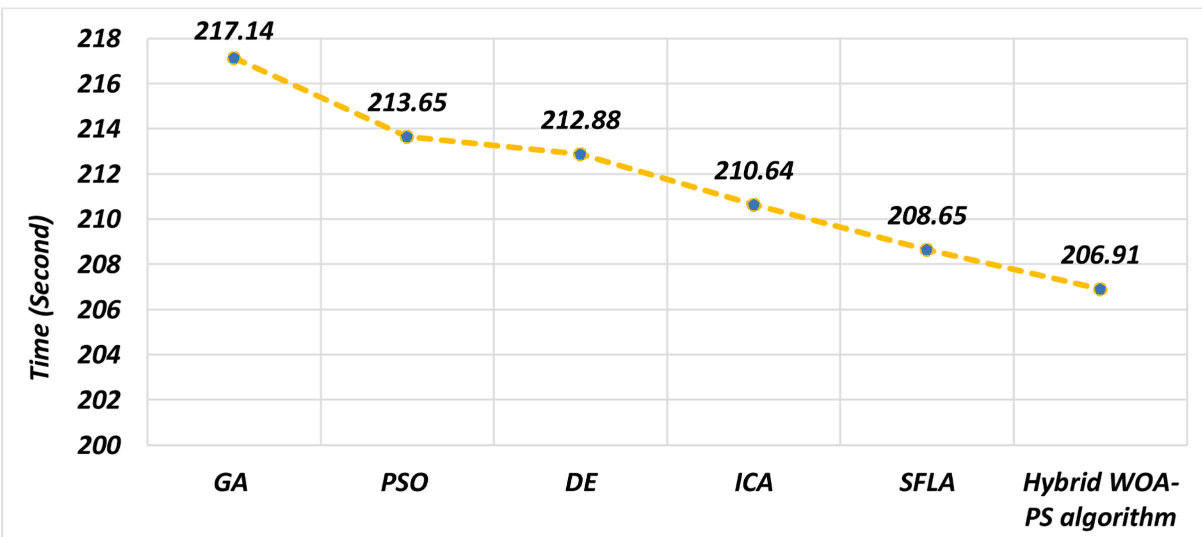

9(d)

Fig. 9. (*continued*).

Table 8
Comparative results (Hot cloudy day).

Algorithm	Best	Worst	Average	Std
GA	263.2377	299.3541	281.3643	16.874
PSO	261.6141	294.1289	279.6643	15.524
DE	261.0874	293.8163	276.1278	15.0650
ICA	258.9579	293.0745	275.2861	14.9572
SFLA	258.0517	292.3372	274.1080	13.0874
Hybrid WOA-PS algorithm	256.7912	291.6357	273.1782	12.661

Instead of using data from only one day, as has been done in other published works, this research analyzes the effects of seasonal weather conditions on PV power generation and day-ahead scheduling by using data from four days spread over the year. While it is assumed that temperature does not change throughout the year, the effects of different weather conditions have been analyzed and applied to the problem by making use of actual data from the NREL (National Renewable Energy Laboratory) [45]. Accordingly, the days are categorized into four groups: cold sunny, cold cloudy, hot sunny, and hot cloudy. Tables 4 and 5 represent the solar irradiance profile for these four days, where GHI stands for the global horizontal irradiance, stated as the sum of ground-reflected irradiation, direct normal irradiance (DNI), and diffuse horizontal irradiation (Diff). Diff is defined as the irradiation components that clouds or any other objects transmit. DNI shows the directed sunlight. It should be noted that the amount of irradiance, reflected from the ground is significantly lower than other items and it can be ignored in the calculations.

It is noteworthy that contrary to the research studies, carried out before, considering only one day of the year for characterizing the PV power generation, this paper presents a comprehensive simulation by modeling the seasonal weather conditions. Accordingly, the PV power generation for these four days (hot-sunny (HS), cold-sunny (CS), hot-cloudy (HC), and cold-cloudy (CC)) have been obtained and depicted in Fig 7. The parameter settings of HWOA-PS as represented in Appendix A.

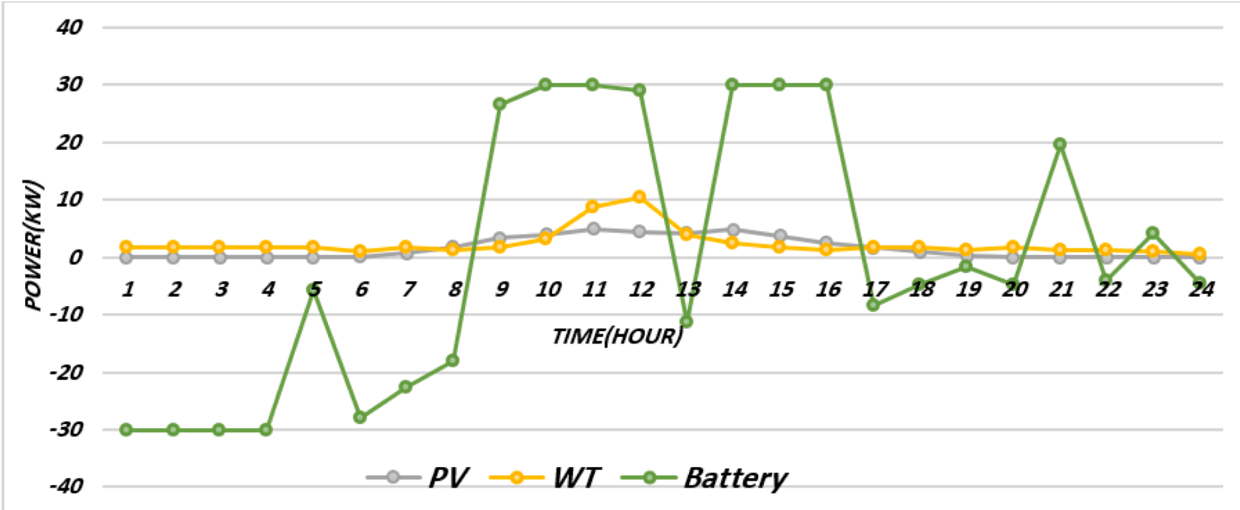

10(a)

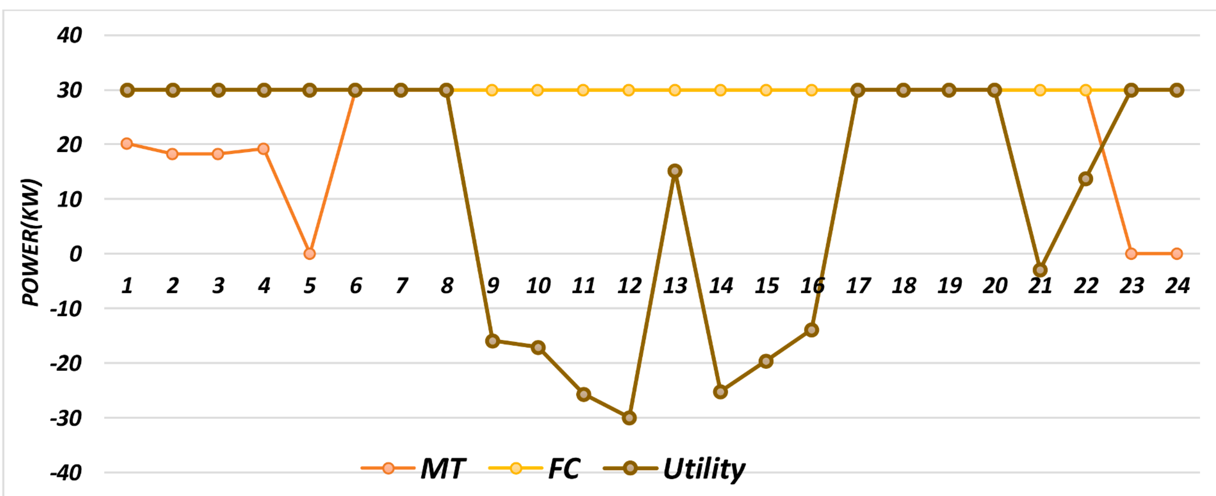

10(b)

Fig. 10. (a) and (b). Hourly dispatch results, reported by the HWOA-PS algorithm (Hot Cloudy day); (c) Battery's charging/discharging; (d) Mean simulation time.

6.1. Case 1

The day-ahead operation problem of the MG is tackled in this section, and Table 6 includes the results, obtained for a warm sunny day. The results, derived by using the presented HWOA-PS show the more desired performance of this hybrid algorithm, compared to the GA, PSO, DE [36], ICA [37], and SFLA [38]. In this regard, four indices have been employed to make a fair comparison between these methods. As Figs. 8 (a) and 8(b) illustrate, the MT would contribute less to supplying the load demand in this day, mainly because of its relatively high operating cost. During time intervals 9 to 17, the decision-maker preferred to mitigate the power, absorbed from the upstream system because of its relatively high cost, and operate FC and MT at the nominal capacity while the PV panel also generates more. As a result, any surplus power generation can be injected into the grid. It is also noted that the MT is accounted as one of the promising options to supply the peak load demand in comparison with the upstream grid.

Moreover, Fig. 8(a) and 8(b), and 8(c) depict the share of each asset in supplying the load demand, where the BEES unit absorbs low-price power from the grid during hours 0 to 8 and 16 to 20 while it supplies merely 1.9% of the demand.

The proposed optimization algorithm's computational effectiveness has been evaluated in this study, where the Hybrid WOA-PS algorithm's average solution time is contrasted with that of other approaches. The results demonstrate that the mean simulation time required by the suggested hybrid Hybrid WOA-PS algorithm technique in Case 1 is 110.34 s, while the time required by the other techniques including GA, PSO, DE, ICA, and SFLA approaches is 119.44 s, 117.21 s, 115.64 s, 114.32 s, and 112.37 s, respectively. As a result, the time needed by the Hybrid WOA-PS algorithm is significantly less than that of other approaches, as depicted in Fig. 8. (d).

6.2. Case 2

The problem is solved by using the data of the cold sunny day, where the power output of the PV panel shows a smaller amount of power generation compared to the hot sunny day mainly due to the lower amount of solar irradiance. The results have been shown in Table 7. The hourly dispatch of units, reported by the proposed HWOA-PS, is shown in Figs. 9(a) and 9(b). Fig. 9(b) shows that the amount of power,

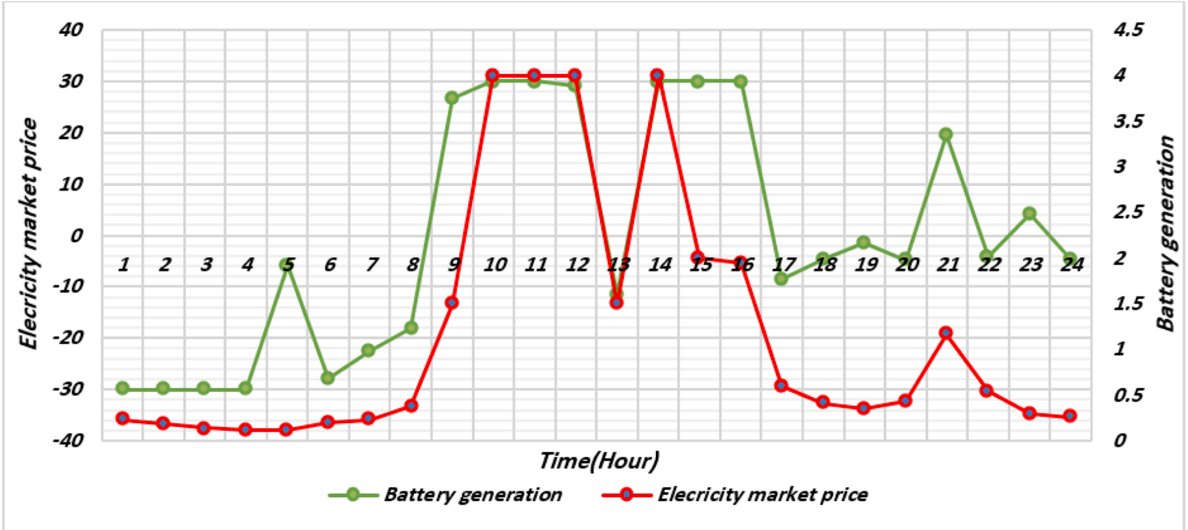

10(c)

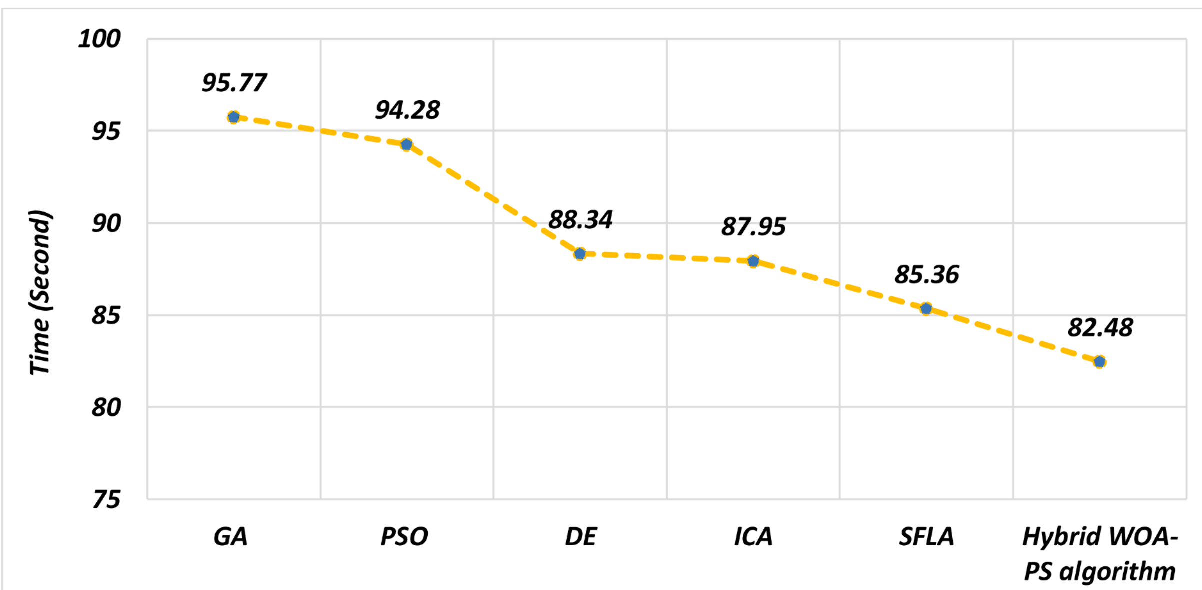

10(d)

Fig. 10. (*continued*).

Table 9
Comparative results, derived from different methods for the cold cloudy day.

Algorithm	Best	Worst	Average	Std
GA	259.0694	333.2495	273.7717	20.5842
PSO	257.4357	331.1718	272.3484	18.7612
DE	255.3791	330.2856	271.9522	16.9641
ICA	254.9876	328.6418	270.1727	15.3378
SFLA	254.0784	328.0874	269.9829	14.2297
Hybrid WOA-PS algorithm	253.135	326.0155	269.3611	13.7215

absorbed from the utility grid is significantly lower than the warm sunny day, leading to reduced operating cost. The battery absorbs low-price power to charge over intervals 1 to 7 as shown in Fig. 9(c), while utilizing the MT to supply the charging power of the BEES is reasonable. As Fig. 9(a) shows, the battery injects power to the system during intervals 9 to 16. Furthermore, a smaller amount of energy is delivered to the utility grid as the PV panel generates lower power. The MT and FC units also have the highest contribution to supplying the load demand.

Fig. 9 shows how long it took for each algorithm to resolve the case study that was provided in Fig. 9(d). This graph shows how the suggested framework takes 4206.911 s to solve the problem in the second case study, which is much less time than the GA, PSO, and ICA algorithms, which take 217.14 s, 213.65 s, and 114.32 s, respectively.

6.3. Case 3

The data of the hot cloudy day are used in this section to simulate the problem and assess the effects of weather conditions on the operation of the MG. As Table 8 represents, the HWOA-PS has resulted in a reduced cost compared to other methods, and the hourly dispatch of assets is illustrated in Figs. 10. Due to the lower amount of solar irradiance, available during this cloudy day, the amount of power, produced by the PV is considerably low. Besides, the MT is used less, and accordingly, the power injected to the upstream grid has become significantly low compared to the previous two cases. The BEES unit also delivers power

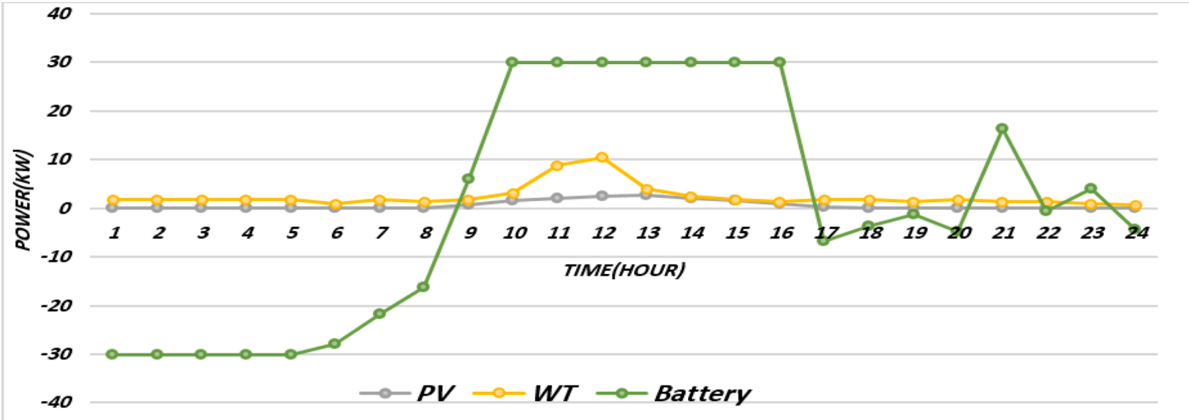

11(a)

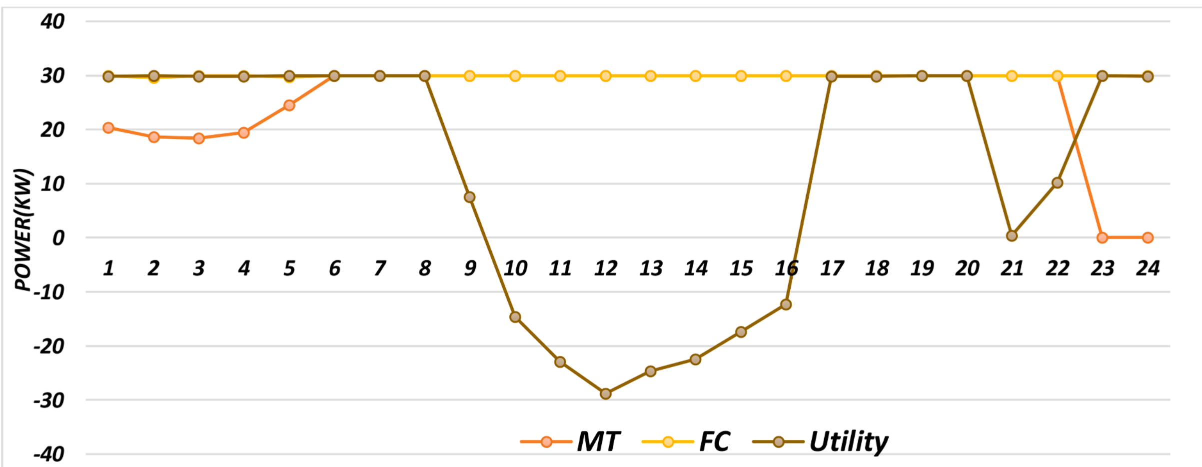

11(b)

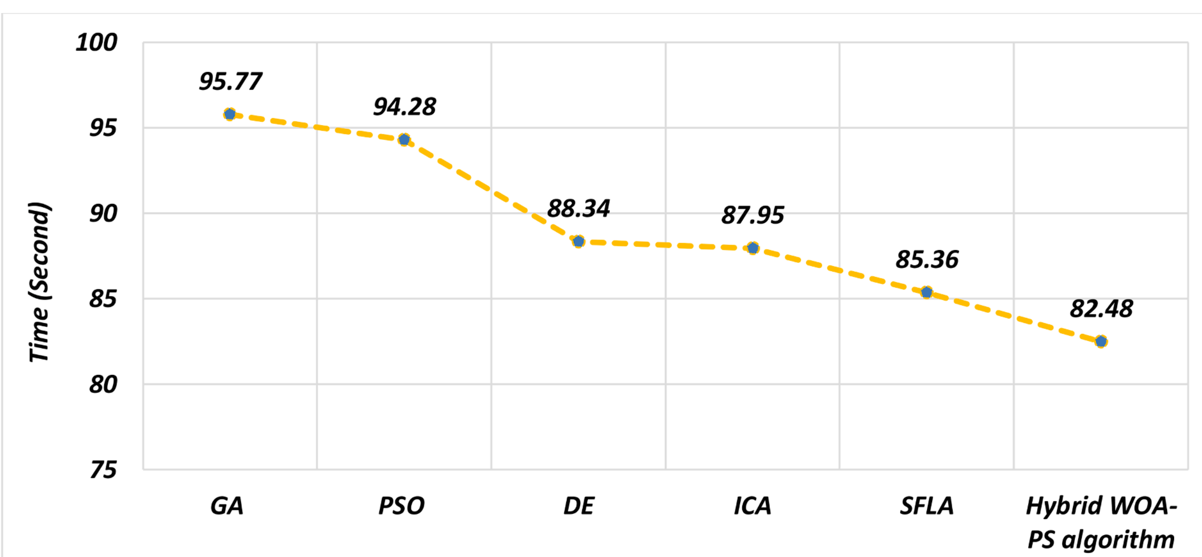

11(c)

Fig. 11. (a) and (b). Hourly dispatch results, reported by the HWOA-PS algorithm (Cold cloudy day); (c) Mean simulation time.

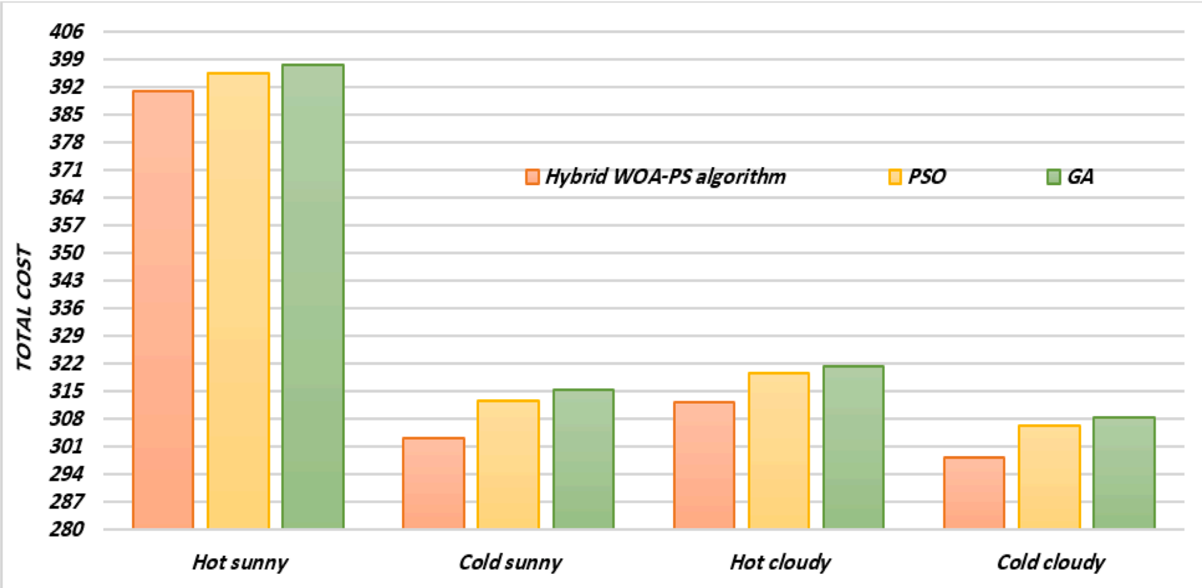

Fig. 12. Total operating cost.

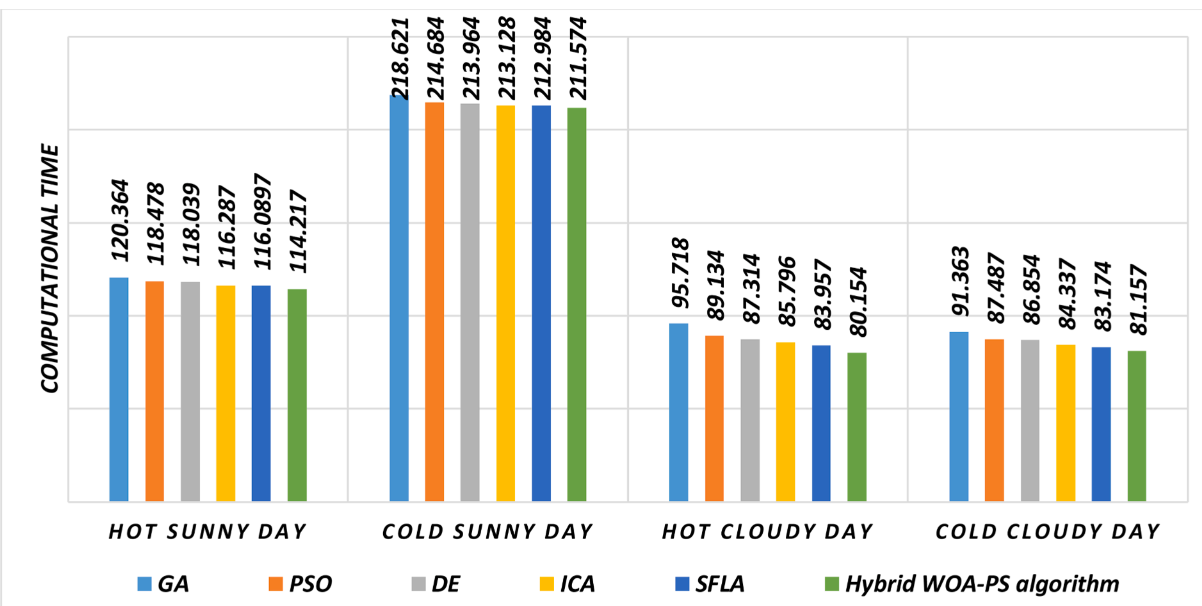

Fig. 13. Response time.

Table 10
Number of hits to achieve the best solution.

Algorithms	Case 1	Case 2	Case 3	Case 4
HWOA -PS	37	38	37	37
SFLA	34	33	31	33
ICA	31	30	31	31
DE	33	34	33	32
PSO	32	31	31	32
GA	31	32	31	30

to the system during intervals 9 to 16 shown in Fig. 10(c). As Fig. 10(b) depicts, the MT and FC units with the lowest operating costs generate more power compared to other assets.

Fig. 10 shows how long it took for each algorithm to resolve the case study that was provided in Fig. 10(d). This chart shows how much faster the proposed method, which takes 82.48 s to solve the problem under study, is than the GA, PSO, and ICA methods.

6.4. Case 4

The cold cloudy day is simulated in this section and the impacts of weather conditions of this day have been assessed. The results, obtained by using the HWOA-PS are represented in Table 9. As this table shows, the presented HWOA-PS has led to a more desired solution, compared to other algorithms. Moreover, due to the cloudy weather conditions, the amount of power, generated by the PV system is considerably low, as shown in Figs. 11. The operating cost, obtained for the cold cloudy day is lower compared to other days. During the first eight intervals, the BEES unit absorbs power to charge to its nominal capacity, while it delivers power until interval 16. The power generation of the MT is maximum and other DGs besides the upstream network supply the load demand. The major part of the load demand is supplied by the FC and MT, as illustrated in Fig. 11(b).

Fig. 11(c) shows how long it took for each method to solve the given case study. As shown in this figure, the proposed method takes 82.48 s to solve the problem under study, a period that is significantly less than that required by the GA, PSO, and ICA methods.

Tables 6–9 represent the comparative results in terms of the four metrics. It has been found that the operating cost of a hot sunny day would be more than the cold sunny day due to the higher PV power generation in spring with longer days. Likewise, the clod cloudy day and hot cloudy day can also be compared. In general, the cost for the hot cloudy day is more than the cold cloudy day due to the higher values of solar irradiance with a longer day. Fig. 12 depicts the total operating cost for 40 trails. As can be observed, considering the uncertain parameters has led to increasing the operating cost and Fig. 13 shows the time response for 40 trails for the sake of comparison between the optimization methods. The results obtained for the single-objective optimization problem tackled using the HWOA-PS method, show that this method is a highly reliable method.

The hybrid HWOA-PS algorithm suggested for any of the four cases involving 40 trials is evaluated in this section. According to Table 10, the number of trails for the HWOA-PS algorithm to find the optimal solution is 37 out of a total of 40. Consequently, this algorithm has a success rate of 96% in tackling the MG's day-ahead operation problem. Other methods have substantially lower success rates. The obtained results indicate that the hybrid HWOA-PS algorithm is associated with superior performance, and is computationally prominent and robust. In addition, the proposed hybrid HWOA-PS algorithm has a shorter average simulation time than other approaches in tackling the MG's day-ahead resource scheduling problem. This analysis demonstrates that the hybrid HWOA-PS method is superior to other approaches.

7. Conclusion

The paper investigated the problem of the day-ahead stochastic operation of an MG in the presence of BEES system, renewable energies, and non-renewable energy resources. There were a PV panel, a WT, an FC, and an MT that all contributed to the power generation. A stochastic optimization model with a single objective was developed for the problem, and the HWOA-PS was presented to be used to solve the optimization problem. Furthermore, four different days were simulated throughout the year as opposed to single-day modeling to account for the fluctuating weather conditions. Operating cost on a warm sunny day, was 351.1964 €ct, on a cold sunny day, it was 284.2851 €ct, on a warm cloudy day, it was 256.791 €ct, and on a cold cloudy day, it was 253.135 €ct, as derived by the supplied HWOA-PS. The provided method outperformed both the GA and the PSO in a comprehensive comparison, and it also outperformed the PSO, DE, ICA, and SFLA. Future work investigates the optimal operation of MGs while implementing demand response programs using a robust optimization framework. Furthermore, the influence of EV charging stations would be covered. To provide a more accurate assessment of the problem, a close-to-real-time resource scheduling paradigm will be proposed.

CRediT authorship contribution statement

Tao Hai: Methodology, Writing – original draft, Software, Validation, Formal analysis, Writing – review & editing. **Jincheng Zhou:** Methodology, Writing – original draft, Software, Validation, Formal analysis, Writing – review & editing. **Kengo Muranaka:** Methodology, Writing – original draft, Software, Validation, Formal analysis.

Declaration of Competing Interest

The authors declare that they have no known competing financial interests or personal relationships that could have appeared to influence the work reported in this paper. The authors declare the following financial interests/personal relationships which may be considered as potential competing interests:

Data availability

No data was used for the research described in the article.

Acknowledgments

This work was supported by the National Natural Science Foundation of China (No.61862051), the Science and Technology Foundation of Guizhou Province (No.[2019]1299, No.ZK[2022]550), the Top-notch Talent Program of Guizhou province (No.KY[2018]080), the Natural Science Foundation of Education of Guizhou province(No.[2019]203) and the Funds of Qiannan Normal University for Nationalities (No. qnsy2018003, No. qnsy2019rc09, No. qnsy2018JS013, No. qnsyrc201715).

Appendix A

Maximum iteration of HWOA-PS=150 for both algorithms.
Mesh size of 1
Mesh expansion factor= 2
Mesh contraction factor =0.5
All tolerances=10^{-6}

References

[1] A. Bolurian, H. Akbari, S. Mousavi, Day-ahead optimal scheduling of microgrid with considering demand side management under uncertainty, Electr. Power Syst. Res. 209 (2022 Aug 1), 107965.
[2] A. Azarhooshang, D. Sedighizadeh, M. Sedighizadeh, Two-stage stochastic operation considering day-ahead and real-time scheduling of microgrids with high renewable energy sources and electric vehicles based on multi-layer energy management system, Electr. Power Syst. Res. 201 (2021 Dec 1), 107527.
[3] A. Ouammi, Y. Achour, H. Dagdougui, D. Zejli, Optimal operation scheduling for a smart greenhouse integrated microgrid, Energy Sustain. Dev. 58 (2020 Oct 1) 129–137.
[4] Sustainable microgrids: economic, environmental and social costs and benefits of microgrid deployment.
[5] E.M. Ahmed, M. Aly, A. Elmelegi, A.G. Alharbi, Z.M. Ali, Multifunctional distributed MPPT controller for 3P4W grid-connected PV systems in distribution network with unbalanced loads, Energies 12 (24) (2019 Jan) 4799.
[6] M. Khaksar, A. Rezvani, M.H. Moradi, Simulation of novel hybrid method to improve dynamic responses with PSS and UPFC by fuzzy logic controller, Neural Comput. Appl. 29 (3) (2018 Feb 1) 837–853.
[7] S. Dadfar, K. Wakil, M. Khaksar, A. Rezvani, M.R. Miveh, M. Gandomkar, Enhanced control strategies for a hybrid battery/photovoltaic system using FGS-PID in grid-connected mode, Int. J. Hydrog. Energy 44 (29) (2019 Jun 7) 14642–14660.
[8] K. Mahmoud, M. Abdel-Nasser, E. Mustafa, Z. M Ali, Improved salp–swarm optimizer and accurate forecasting model for dynamic economic dispatch in sustainable power systems, Sustainability 12 (2) (2020 Jan) 576.
[9] M. Izadbakhsh, A. Rezvani, M. Gandomkar, Dynamic response improvement of hybrid system by implementing ANN-GA for fast variation of photovoltaic irradiation and FLC for wind turbine, Arch. Electr. Eng. 64 (2) (2015) 291–314.
[10] Y. Li, S.Q. Mohammed, G.S. Nariman, N. Aljojo, A. Rezvani, S. Dadfar, Energy management of microgrid considering renewable energy sources and electric vehicles using the backtracking search optimization algorithm, J. Energy Resour. Technol. 142 (5) (2020 May 1).
[11] M.H. Mostafa, S.H. Aleem, S.G. Ali, A.Y. Abdelaziz, P.F. Ribeiro, Z.M. Ali, Robust energy management and economic analysis of microgrids considering different battery characteristics, IEEE Access 8 (2020 Mar 18) 54751–54775.
[12] W. Chen, Z. Shao, K. Wakil, N. Aljojo, S. Samad, A. Rezvani, An efficient day-ahead cost-based generation scheduling of a multi-supply microgrid using a modified krill herd algorithm, J. Clean. Prod. 272 (2020 Nov 1), 122364.
[13] M. Abedini, M. Abedini, Energy management and control policies of the islanded microgrids, Sustain. Cities Soc. 38 (2018 Apr 1) 714–722.
[14] A. Rezvani, M. Gandomkar, M. Izadbakhsh, A. Ahmadi, Environmental/economic scheduling of a micro-grid with renewable energy resources, J. Clean. Prod. 87 (2015 Jan 15) 216–226.
[15] R. Hemmati, H. Mehrjerdi, S.M. Nosratabadi, Resilience-oriented adaptable microgrid formation in integrated electricity-gas system with deployment of multiple energy hubs, Sustain. Cities Soc. (2021 Apr 19), 102946.

[16] A. Aldosary, M. Rawa, Z.M. Ali, A. Razmjoo, A. Rezvani, Energy management strategy based on short-term resource scheduling of a renewable energy-based microgrid in the presence of electric vehicles using θ-modified krill herd algorithm, Neural Comput. Appl. (2021 Feb 14) 1–6.
[17] J. Aghaei, M.I. Alizadeh, Multi-objective self-scheduling of CHP (combined heat and power)-based microgrids considering demand response programs and ESSs (energy storage systems), Energy 55 (2013 Jun 15) 1044–1054.
[18] A. Chaouachi, R.M. Kamel, R. Andoulsi, K. Nagasaka, Multiobjective intelligent energy management for a microgrid, IEEE Trans. Ind. Electron. 60 (4) (2012 Feb 24) 1688–1699.
[19] B. Zhao, Y. Shi, X. Dong, W. Luan, J. Bornemann, Short-term operation scheduling in renewable-powered microgrids: a duality-based approach, IEEE Trans. Sustain. Energy 5 (1) (2013 Sep 30) 209–217.
[20] D. Quiggin, S. Cornell, M. Tierney, R. Buswell, A simulation and optimisation study: towards a decentralised microgrid, using real world fluctuation data, Energy 41 (1) (2012 May 1) 549–559.
[21] A. Kavousi-Fard, T. Niknam, M. Fotuhi-Firuzabad, Stochastic reconfiguration and optimal coordination of V2G plug-in electric vehicles considering correlated wind power generation, IEEE Trans. Sustain. Energy 6 (3) (2015 Apr 15) 822–830.
[22] Z. Shao, D.J. Armaghani, B.Y. Bejarbaneh, M.A. Mu'azu, E.T Mohamad, Estimating the friction angle of black shale core specimens with hybrid-ANN approaches, Measurement 145 (2019 Oct 1) 744–755.
[23] N.E. Koltsaklis, M. Giannakakis, M.C. Georgiadis, Optimal energy planning and scheduling of microgrids, Chem. Eng. Res. Des. 131 (2018 Mar 1) 318–332.
[24] M. Sedighizadeh, M. Esmaili, N. Mohammadkhani, Stochastic multi-objective energy management in residential microgrids with combined cooling, heating, and power units considering battery energy storage systems and plug-in hybrid electric vehicles, J. Clean. Prod. 195 (2018 Sep 10) 301–317.
[25] F.H. Aghdam, S. Ghaemi, N.T. Kalantari, Evaluation of loss minimization on the energy management of multi-microgrid based smart distribution network in the presence of emission constraints and clean productions, J. Clean. Prod. 196 (2018 Sep 20) 185–201.
[26] T. Khalili, A. Jafari, E. Babaei, Scheduling and siting of storages considering power peak shaving and loss reduction by exchange market algorithm, in: In2017 Smart Grid Conference (SGC), IEEE, 2017 Dec 20, pp. 1–7.
[27] S.M. Mortazavi, N. Shiri, M.S. Javadi, S.D. Dehnavi, Optimal planning and management of hybrid vehicles in smart grid, Ciência e Natura 37 (2015 Dec 19) 253–263.
[28] A.A. Moghaddam, A. Seifi, T. Niknam, Multi-operation management of a typical micro-grids using particle swarm optimization: a comparative study, Renew. Sustain. Energy Rev. 16 (2) (2012 Feb 1) 1268–1281.
[29] O. Hafez, K. Bhattacharya, Optimal planning and design of a renewable energy based supply system for microgrids, Renew. Energy 45 (2012 Sep 1) 7–15.
[30] R. Chedid, S. Rahman, Unit sizing and control of hybrid wind-solar power systems, IEEE Trans. Energy Convers. 12 (1) (1997 Mar) 79–85.
[31] H. Morais, P. Kádár, P. Faria, Z.A. Vale, H.M. Khodr, Optimal scheduling of a renewable micro-grid in an isolated load area using mixed-integer linear programming, Renew. Energy 35 (1) (2010 Jan 1) 151–156.
[32] A.G. Tsikalakis, N.D. Hatziargyriou, in: Centralized control for optimizing microgrids operation. In2011 IEEE power and energy society general meeting, IEEE, 2011 Jul 24, pp. 1–8.
[33] Y.H. Chen, S.Y. Lu, Y.R. Chang, T.T. Lee, M.C. Hu, Economic analysis and optimal energy management models for microgrid systems: a case study in Taiwan, Appl. Energy 103 (2013 Mar 1) 145–154.
[34] G.C. Liao, Solve environmental economic dispatch of Smart MicroGrid containing distributed generation system–Using chaotic quantum genetic algorithm, Int. J. Electr. Power Energy Syst. 43 (1) (2012 Dec 1) 779–787.
[35] R.K. Khadanga, S. Padhy, S. Panda, A. Kumar, Design and analysis of multi-stage PID controller for frequency control in an islanded micro-grid using a novel hybrid whale optimization-pattern search algorithm, Int. J. Numer. Model. Electron. Netw. Devices Fields 31 (5) (2018 Sep) e2349.
[36] M. Durairasan, D. Balasubramanian, An efficient control strategy for optimal power flow management from a renewable energy source to a generalized three-phase microgrid system: a hybrid squirrel search algorithm with whale optimization algorithm approach, Trans. Institute of Measurement and Control (2020 Feb 6), 0142331220901628.
[37] L.A. Wong, V.K. Ramachandaramurthy, S.L. Walker, P. Taylor, M.J. Sanjari, Optimal placement and sizing of battery energy storage system for losses reduction using whale optimization algorithm, J. Energy Storage 26 (2019 Dec 1), 100892.
[38] K. Kasturi, M.R. Nayak, Optimal planning of charging station for EVs with PV-BES unit in distribution system using WOA, in: In2017 2nd International Conference on Man and Machine Interfacing (MAMI), IEEE, 2017 Dec 21, pp. 1–6.
[39] X. Ge, F.W. Ahmed, A. Rezvani, N. Aljojo, S. Samad, L.K. Foong, Implementation of a novel hybrid BAT-Fuzzy controller based MPPT for grid-connected PV-battery system, Control Eng. Pract. 98 (2020 May 1), 104380.
[40] D. Wu, G.S. Nariman, S.Q. Mohammed, Z. Shao, A. Rezvani, S. Mohajeryami, Modeling and simulation of novel dynamic control strategy for PV–wind hybrid power system using FGS− PID and RBFNSM methods, Soft Comput. (2019 Oct 10) 1–23.
[41] J. Aghaei, M. Karami, K.M. Muttaqi, H.A. Shayanfar, A. Ahmadi, MIP-based stochastic security-constrained daily hydrothermal generation scheduling, IEEE Syst. J. 9 (2) (2013 Nov 22) 615–628.
[42] S. Mirjalili, A. Lewis, The whale optimization algorithm, Adv. Eng. Softw. 95 (2016 May 1) 51–67.
[43] S. Yin, J. Cagan, An extended pattern search algorithm for three-dimensional component layout, J. Mech. Des. 122 (1) (2000 Mar 1) 102–108.
[44] Bao Y., Hu Z., Xiong T. A PSO and pattern search based memetic algorithm for SVMs parameters optimization. Neurocomputing.
[45] B. Marion, B. Kroposki, K. Emery, J. Del Cueto, D. Myers, C. Osterwald, Validation of a photovoltaic module energy ratings procedure at NREL, Nat. Renew. Energy Lab., Golden, CO (US) (1999 Aug 11).